17 Lecture 17. Billiards

N. Chernov and R. Markarian, *Chaotic Billiards* (Mathematical Surveys and Monograph 127, AMS, 2006).

17.1 Billiard

Let Q be a compact subset of E^d (d-Euclidean space)[169] with piecewise smooth boundary. The time evolution T^t of a particle traveling according to the following rules is called a billiard in Q:
(1) A single particle moves with speed 1 along the geodesic (= straight line) if it is away from ∂Q.
(2) When the particle hits the boundary, the specular reflection is assumed.
Technically, we assume that at almost all points in Q the particle hits ∂Q within a finite time except for zero measure direction subsets of S^{d-1}.[170]

The phase space of the system is $M = \{(q, v) \,|\, q \in Q, v \in S^{d-1}\}$. The ordinary d-Lebesgue measure $\times$ the Riemann volume of S^{d-1} is an invariant measure (= phase volume) of the billiard.

You could imagine Q as a room whose wall(s) ∂Q is made of mirrors. The dynamics we wish to study is the geometrical optics i the room.
cf. Illumination problem:
https://www.youtube.com/watch?v=xhj5er1k6GQ&frags=wn

17.2 Ambrose-Kakutani representation

Since the particle of a billiard travels at speed 1 between collisions with ∂Q, we can describe the dynamics of the particle with the initial condition $x = (q, n)$ ($q \in \partial Q$ and $n \in S^{d-1}$) as a sequence of collisions with ∂Q. Thus we can describe the dynamics by a map T from ∂M ($= \partial Q \times S^{d-1}$) into itself and the needed time for the travel between successive collisions: $\tau(x)$. Here, T is defined by $x_{k+1} = Tx_k$, where $x_k = (q_k, n_k)$ ($q_k \in \partial Q$, $n_k \in S^{d-1}$) is the position and the velocity immediately after

[169] A mathematically more general definition uses d-Riemannian manifold, instead.
[170] ∂Q can contain non-differentiable subsets (called the singular components of the boundary), but we ignore them. We will not define dynamics if the particle hits these subsets.

the k-th collision (see Fig. 17.1).

Notice that this representation corresponds to the suspension of the Poincaré map.

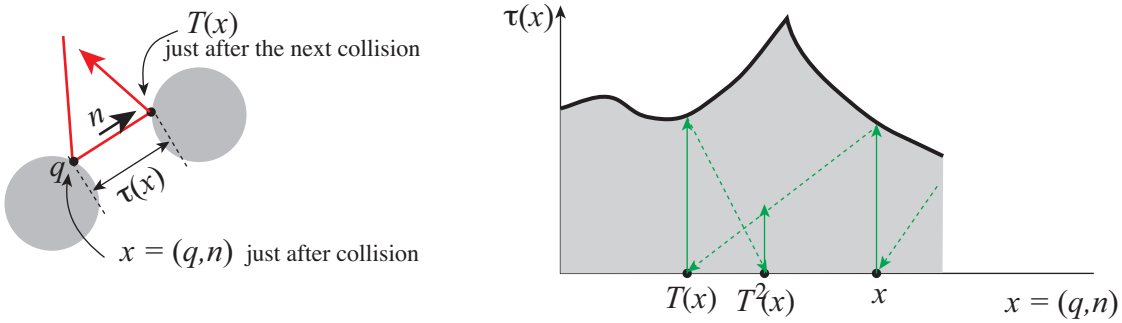

Figure 17.1: Ambrose-Kakutani representation

17.3 Polygonal or polyhedral billiards

If Q is a polygon, then we can consider a map $\sigma : S^1 \to S^1$, the directional portion of the Ambrose-Kakutani representation of the billiard. We can define a reflection at the i-th boundary component (edge or surface hyperplane) as a map $\sigma_i : S^{d-1} \to S^{d-1}$. n collisions may be expressed as a map $\sigma_{i_n}\sigma_{i_{n-1}} \cdots \sigma_{i_2}\sigma_{i_1}$. The totality of such chains define a subgroup G_Q of the isometry of S^{d-1}. If this is a finite group, the system is not ergodic. For example, if Q is a triangle and all the angles are commensurate, then G_Q is finite.[171] If G_Q is finite, the billiard is not ergodic (because S^{d-1} will never be densely traversed).

17.4 Billiards in polyhedra cannot be chaotic

If Q is a polyhedron, there cannot be any exponential spreading of the trajectories, so it cannot be chaotic (its Kolmogorov-Sinai entropy is zero as we will see later).

For an arbitrary polyhedron (or even polygon) the ergodicity of billiards is not generally understood.

Periodic orbits?: https://www.youtube.com/watch?v=AGX0cLbHaog

17.5 Square billiard

Suppose Q is a square (or a flat T^2). Then, we can visualize the motion with a line

[171] An analogous assertion holds for any polygon.

on the universal covering space (Fig. 17.2)

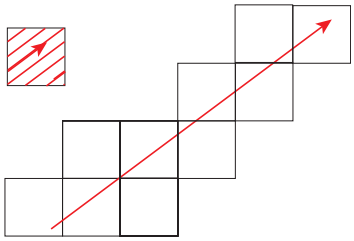

Figure 17.2: A trajectory of a square billiard on the universal covering space

Thus, if the slope is rational, the trajectory is periodic, but if irrational, the trajectory densely cover Q (Weyl's theorem), BUT it is not ergodic, since the velocities make a finite point set.

17.6 Billiards with smooth ∂Q

If Q is a 2-disk (thus, $\partial Q = S^1$), then all the successive reflection points are equally spaced and the angle of reflection is constant. There is a caustic (Fig. 17.3): a caustics is a smooth closed curve γ such that if one segment of the trajectory is tangent to γ all other segments of the same trajectory are also tangent to γ.

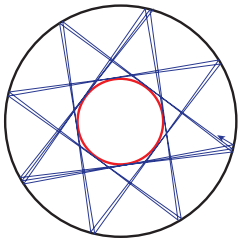

Figure 17.3: A caustic of a circular billiard

Lazutkin showed that if ∂Q is convex and smooth enough (say, C^5), then the totality of caustics is with positive measure (and obviously the system is not ergodic).

Remark If there is a caustics, then there is Dirichlet eigenvalues for $\Delta\psi = \lambda\psi$ that are localized near the caustic (e.g., whisper modes). Shnirelman proved that ψ spreads all over Q in the $\lambda \to \infty$ limit, if the billiard is ergodic.[172]

Fun video: Elliptic pool table https://www.youtube.com/watch?v=3WHBlPvK3Ek&

[172] Bunimovich p156.

frags=wn

In general anything seems to happen:
cardioid billiard: https://www.youtube.com/watch?v=eQfh0gaU4NE

17.7 Dispersing or Sinai billiards[173]

If the boundary ∂Q is inwardly convex at its regular points, the billiard is called a dispersing (or Sinai) billiard.
How dispersive can be seen from:
https://www.youtube.com/watch?v=C1iuNH_99v8 .

Its comparison with a circular billiard is interesting: https://www.youtube.com/watch?v=dI4WuafBF-w&index=4&list=PL2wfI-9_pR8AvNGxOwpfEO7fyS-giW2Ob&frags=wn

The simplest example is $Q = T^2 \setminus$ 2-disk (Fig. 17.4)

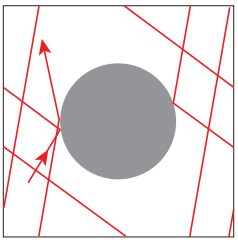

Figure 17.4: Sinai billiard table

Unfortunately, there is no good video for the simplest billiard.

Theorem. Sinai billiards are ergodic and K.

What is K? Roughly,....
There is a finite partition of its phase space $\{A_i\}$ such that almost all the points in M and their coding $x \to \{x_k\}$ according to the rule $T^n(x) \in A_i as x_n = i$ is one-to-one correspondent, the system is called a K-system.

17.8 Why Sinai billiards are chaotic

Here, we use the word 'chaotic' intuitively to mean that the spread of the velocity vectors increases exponentially in time on the average. At each reflection with ∂Q

[173] B. A. Friedman, *The Billiard Problem* (UIUC Physics Thesis, 1985) contains a friendly introduction to the topic.

spread the directions, and, generically speaking, the number of collisions increases linearly with time, so we can expect exponential spreading of the propagation directions on the average in time. Thus, we can expect the system is chaotic.

We can be more quantitative.

17.9 Local time evolution of velocity curvature by propagation
Take a smooth curve passing through $x_0 \in Q$ and assume it is the curve perpendicular to the trajectories. The curvature $\kappa(x_0) = d\varphi/dr$ describes how spread the velocities are (notice that $1/\kappa$ is the curvature radius).

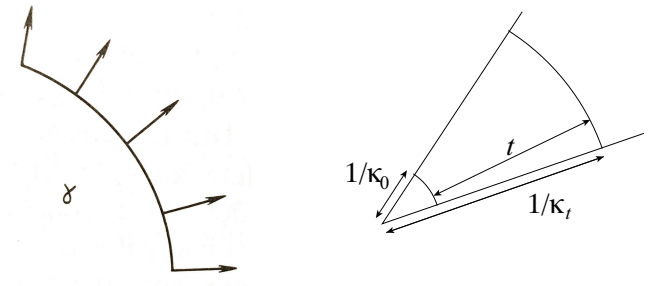

Figure 17.5: A propagation front and the velocities; here γ is a curve in M (not in Q) consisting of a curve $\tilde{\gamma}$ in Q + the unit velocities in ther normal directions

If there is no collision between time 0 and t,

$$\frac{1}{\kappa(x_t)} = t + \frac{1}{\kappa(x_0)}, \tag{17.1}$$

so

$$\kappa(x_t) = \frac{\kappa(x_0)}{1 + t\kappa(x_0)}. \tag{17.2}$$

The expansion rate of the base curve $\tilde{\gamma}$ is $1 + t\kappa(0)$.

17.10 Local time evolution of velocity curvature by collision
If there is a collision at time τ, this curvature changes discontinuously between $\tau - 0$ and $\tau + 0$:

$$\kappa(x_{\tau+0}) = \kappa(x_{\tau-0}) + \frac{2k}{\cos\varphi_\tau}, \tag{17.3}$$

where k is the curvature of the colliding surface and φ_τ is the incidence angle. This may be derived as explained below, but it is basically the well-known lens formula $1/f = 1/d_{\mathrm{o}} + 1/d_{\mathrm{i}}$. For the near optical axis rays, $\varphi = 0$ and $f = -2(1/k)$ (the twice radius of the mirror; $-$ because the mirror is convex);

$1/d_{\rm o} = \kappa(x_{\tau-0})$ (real object) and $1/d_{\rm i} = -\kappa(x_{\tau+0})$ (virtual image).

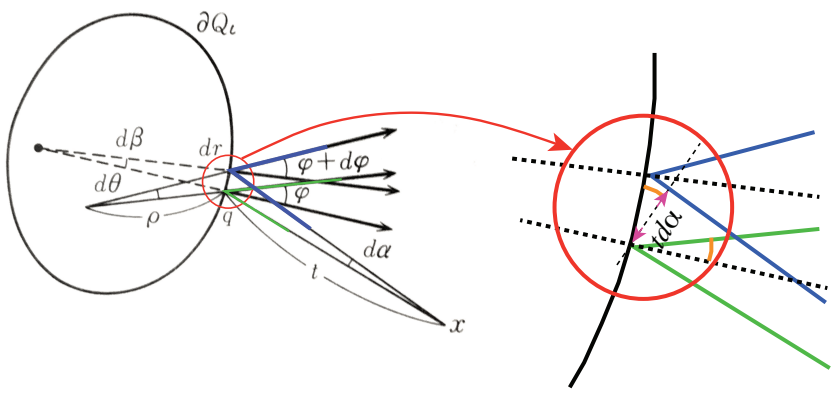

Figure 17.6: A propagation front and the velocities

In Fig. 17.6 the relation between $d\beta$ and $d\alpha$ is

$$\frac{1}{k} d\beta = dr = \frac{t(-d\alpha)}{\cos\varphi_\tau}, \tag{17.4}$$

where α is measured clockwisely while β counterclockwisely, so we need the minus sign. We see

$$d\varphi = 2d\beta - d\alpha, \tag{17.5}$$

because (i) if $d\alpha = 0$, then changing the mirror direction by $d\beta$ changes the reflection angle by $2d\beta$, (ii) if $d\beta = 0$, changing the incidence angle by $d\alpha$ the reflection angle changes by $-d\alpha$. Therefore,

$$d\varphi = 2\frac{kt(-d\alpha)}{\cos\varphi} - d\alpha. \tag{17.6}$$

We know

$$\kappa(x_{\tau-0}) = 1/t = \frac{-1}{\cos\varphi}\frac{d\alpha}{dr}, \quad \kappa(x_{\tau+0}) = \frac{1}{\cos\varphi}\frac{d\varphi}{dr}, \quad k = \frac{d\beta}{dr}. \tag{17.7}$$

Thus, (17.6) reads

$$d\varphi = 2kdr - d\alpha, . \tag{17.8}$$

so we finally obtain (17.3).

17.11 Expansion between successive collisions

The expansion rate of the curve $\tilde{\gamma}$ is, as already seen in **17.9**, $1 + \tau(x_n)k(x_n)$, where $\tau(x_n)$ is time between nth and $n+1$th collisions, and $k(x_n)$ is the curvature just after the nth collision. Notice that from (17.3),

17.12 Relation to geodesics on negative curvature surfaces

The geodesic trajectories near the saddle spread, as is illustrated in

https://www.youtube.com/watch?v=3u2SJKxJhh8&frags=wn after about 11:20

Thus, the geodesic trajectories in the negative curvature Riemannian manifold are exponentially spreading.

Sinai billiards are without any curvature, but what happens at the collision points is just what happens at saddles as illustrated in Fig. 17.7

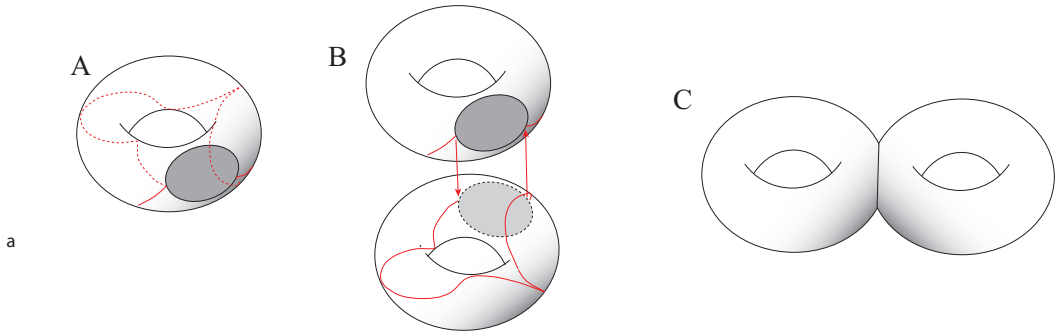

Figure 17.7: 'Saddle' dynamics near ∂Q; here the illustration uses the 'standard' Sinai billiard. A is the torus with a disk scatterer. You can imagine that the particle goes to the 'backside' of the torus upon collision. At the next collision the particle reappears to this side of the world. B: Then, take out the second surface, and connect them to make a 'coupled' T^2. The particles moves 'straight' until it hits the connection ring R; if the ring is 'mollified a bit, it is just a saddle.

17.13 Billiards with focusing elements

Bunimovich proved that billiards on $Q \subset \mathbb{R}^2$ are K, if
(1) ∂Q consists of line segments and parts of circles.
(2) There is no pair of focusing components that are a part of the same circle.
(3) For each circular segment, its completed circle must be in Q.

For example, Qs illustrated in Fig. 17.8 satisfy the above conditions:"

The most famous example is the Bunimovich stadium:

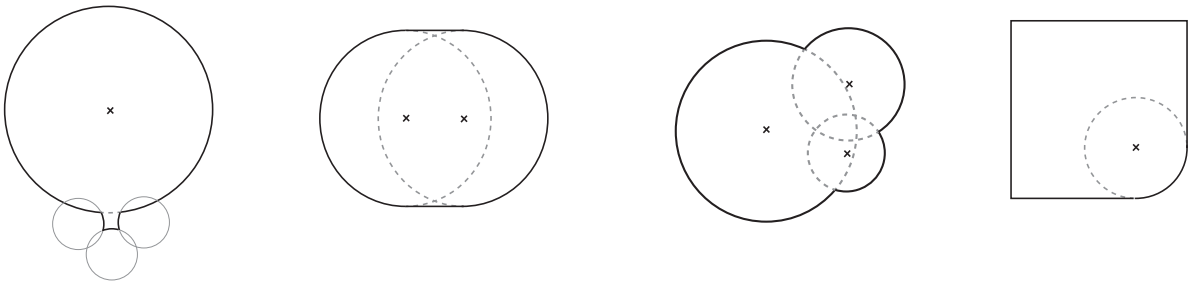

Figure 17.8: Examples of chaotic focusing billiard tables

https://blogs.ams.org/visualinsight/2016/11/15/bunimovich-stadium/.

Remark: the eigenfunction of $\Delta\psi$ on Q are illustrated as
Quantum: https://www.dhushara.com/DarkHeart/QStad/QStad.htm
Bunimovich mitosis http://community.wolfram.com/groups/-/m/t/977013
First 500 eigenmodes: https://youtu.be/3voKV4az0Sk

17.14 Invariant measure of billiards

Since billiards were motivated by Krylov to understand the foundation of statistical mechanics, their probabilistic properties have been of their main interest. There are many different invariant measures (the probability law preserved by dynamics), but the most interesting one is the ones absolutely continuous wrt the Lebesgue measures on the phase space.

Here, I do not discuss what the measure is: it is roughly something like volume. 'Absolute continuity' of a measure ν wrt μ means $\nu(A) = 0$ whenever $\mu(A) = 0$ for any (measurable) set.

From now on we discuss only billiards on 2-dimensional tables Q. The phase space is $\Gamma = Q \times S^1$, where $Q \subset \mathbb{R}^2$. Let us introduce the position coordinates (q_1, q_2) on Q and the angle variable φ to specify the particle velocity during its free time. It should be clear that

$$d\mu = \frac{1}{2\pi|Q|} dq_1 dq_2 d\varphi \tag{17.9}$$

is invariant; this is simply a classical particle system with a constant speed.

17.15 Invariant measure for Ambrose-Kakutani representation

We could introduce an invariant measure on the space shaded in Fig. 17.1 Right. The coordinates we use are q, n and σ, where σ is the vertical coordinate (expressing the

travel distance between successive collisions). Here q may be the coordinate along ∂Q and n may be represented by an angle φ wrt the outward normal on ∂Q. The case of the single disk Sinai billiard on T^2 is illustrated in Fig. 17.9.

Here the small box represents $dq_1 dq_2$. From Fig. 17.9 we see

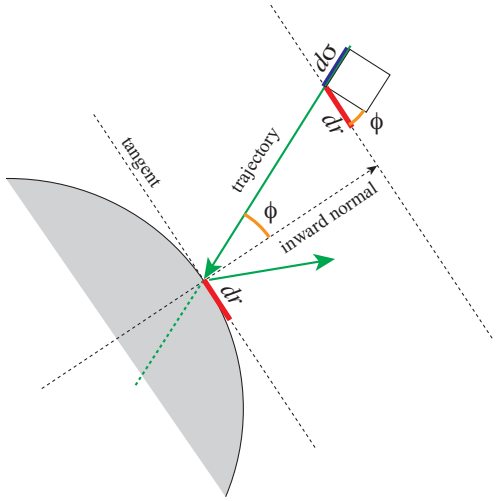

Figure 17.9: The coordinates of the Ambrose-Kakutani representation of 'the' Sinai billiard; notice that $\varphi \in [-\pi/2, \pi/2]$.

$$dq_1 dq_2 = d\sigma dr \cos\varphi. \tag{17.10}$$

Therefore,

$$d\mu \propto \cos\varphi \, d\varphi d\sigma dr. \tag{17.11}$$

We must compute the normalization constant, if μ is a probability measure. For the standard Sinai billiard, the phase volume is $2\pi|Q|$ ($|Q| = 1 - \pi r^2$, if the torus area is 1 and the disc radius is r), so this is the normalization constant.

17.16 Mean free time

The average of $\tau(x)$ for $x \in \Gamma$ is the mean free time. Notice that integral of $d\sigma$ between successive collisions is the free time $\tau(q, n)$. Therefore, for the standard Sinai billiard

$$2\pi|Q| = \int_0^{|\partial Q|} dr \int_{-\pi/2}^{\pi/2} \cos\varphi \, d\varphi \int_0^{\tau(r,\varphi)} d\sigma = \int_0^{|\partial Q|} dr \int_{-\pi/2}^{\pi/2} \cos\varphi \, \tau(r,\varphi) d\varphi \tag{17.12}$$

The mean free time is[174]

$$\langle\tau\rangle = \frac{\int_0^{|\partial Q|} dr \int_{-\pi/2}^{\pi/2} |\cos\varphi| \tau(r,\varphi) d\varphi}{\int_0^{|\partial Q|} dr \int_{-\pi/2}^{\pi/2} |\cos\varphi| d\varphi} \tag{17.13}$$

The denominator is $2\partial Q$. Therefore, we have arrived at

$$\langle\tau\rangle = 2\pi|Q|/2|\partial Q| = (1-\pi r^2)/2r. \tag{17.14}$$

17.17 Abramov formula for the loss of information The Kolmogorov-Sinai entropy (information loss rate per time) h of a billiard may be expressed as

$$h = H/\langle\tau\rangle, \tag{17.15}$$

where H is the entropy change per collision, and $\langle\tau\rangle$ is the mean free time. The formula is called the Abramov formula. That is, a mean field idea works.

It is not hard to see why (17.15) holds. Notice that between collisions there is no loss of information; information is lost only at collisions. Let H_j be the loss of information at the jth collision. Then, its average is H. Let τ_j be the free time before the jth collision. Then, $T = \sum \tau_j$ is needed for the information loss of $\sum H_j$, so

$$h = \frac{\sum H_j}{\sum \tau_j} = \frac{H}{\langle\tau\rangle}. \tag{17.16}$$

17.18 Loss rate of information of billiards
Take a small square as in Fig. 17.10 Left. Suppose the length of its edge is the minimum length that we can discern. Thus we can tell whether a point is in it or not: this answer can be obtained by a single yes-no question. Thus, we get one bit of information.

After a single application of the map T (in our context T) the square is stretched in the unstable manifold direction and compressed in the stable manifold direction.

If we know that the system is in the square now, after applying T we know the system point is near the unstable manifold; more precisely, we know the system is

[174]Here, we assume that the particle can go any where on the table = ergodicity; this needs a proof.

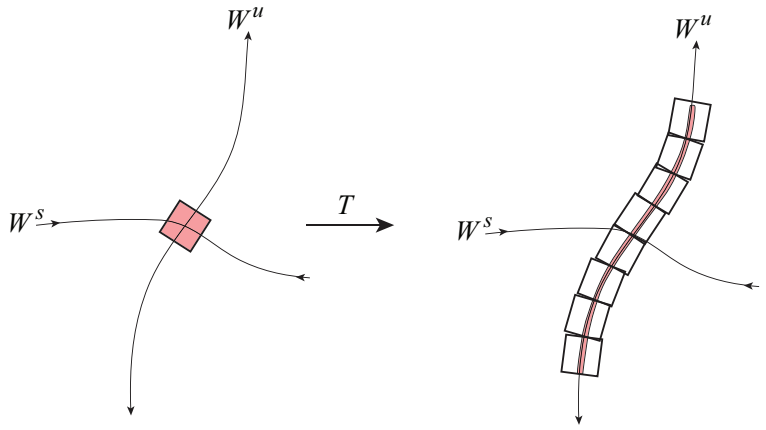

Figure 17.10: Local loss of information due to expansion

in one box which cover the stretched square as in Fig. 17.10 Right. To locate the system as accurately as one time step before, we should choose one box out of 8 boxes. We need 3 bits of information. That is, T dissipated 3 bits of information; our knowledge about the system is lost by 3 bits per one mapping step.

Thus, the log (or $\log_2$) of the expansion rate of the unstable manifold must be the information loss rate, whose 'ensemble average'[175] is called the Kolmogorov-Sinai (KS) entropy h_T, as we will see later.

17.19 Kolmogorov-Sinai entropy of Sinai billiard: introduction

Let $r = \psi(\varphi)$ be the unstable manifold. This is mapped by $T : (r, \varphi) \to (r_1, \varphi_1)$ to $\varphi_1 = \psi_1(r_1)$. Then, the expansion rate m can be computed as

$$m = \frac{\|(dr_1, d\varphi_1)\|}{\|(dr, d\varphi)\|} = \left|\frac{\partial r_1}{\partial r}\right| \frac{\|(1, \partial\varphi_1/\partial r_1)\|}{\|(1, \partial\varphi/\partial r)\|}. \tag{17.17}$$

Let us write μ as the normalized phase volume (invariant measure) (**??**) in **17.14**. Then,

$$h_T = \int d\mu \log m \tag{17.18}$$

$$= \int d\mu \log \left|\frac{dr_1}{dr}\right| + \int d\mu \log \|(1, \partial\varphi_1/\partial r_1)\| - \int d\mu \log \|(1, \partial\varphi/\partial r)\| \tag{17.19}$$

[175] average over the invariant probability measure.

$$= \int d\mu \, \log \left| \frac{dr_1}{dr} \right| . \tag{17.20}$$

We must calculate the derivative: note, however, dr_1/dr is the derivative along the unstable manifold (i.e., φ also changes, when r is changed according to $d\varphi = (d\psi/dr)dr$.

To calculate h_T, we need much more details of the Sinai billiard.

17.20 Domain of T

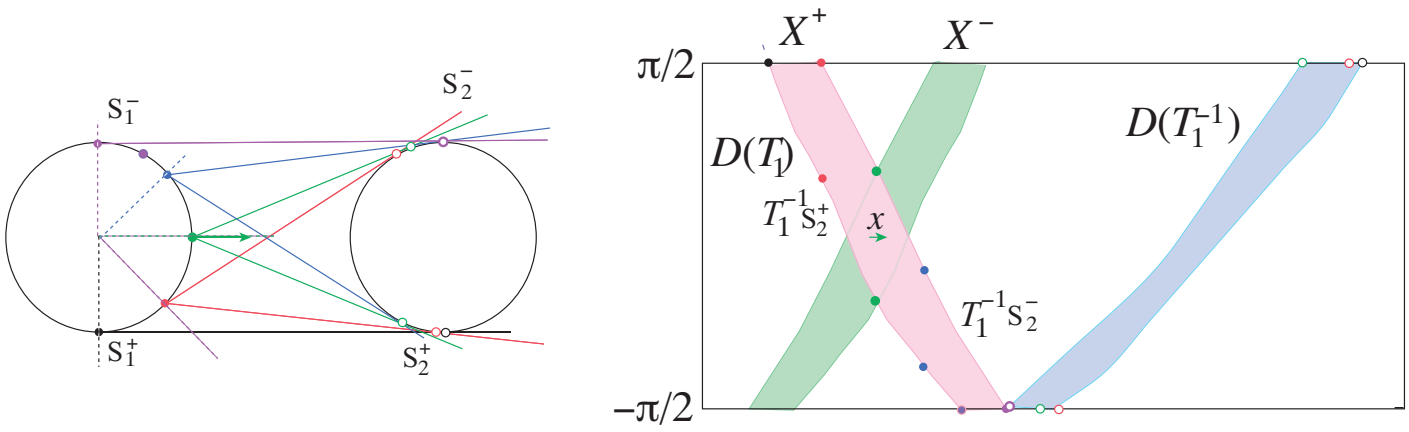

Figure 17.11: The 'Poincaré' map T for the Sinai billiard.

Fig. 17.11 The 'Poincaré' map $T$for the Sinai billiard.
Right: The rectangle shows the boundary ∂M of the phase space (i.e., ∂Q and the velocity vectors (just after collisions into Q direction) there in S^1. The pink band is the domain for T hitting '2' (from '1', '1' and '2' may be the same disk (different sides) shown Left; the colored dots correspond to the starting sites on '1'.
The purple strip is the domain of T^{-1} coming back to '1' from '2'.
The green strip is the domain of T^{-1} from '1', which is definable by the pink strip with the mirroring its velocities with respect to the normal directions (time reversal transformation).
The green arrow x denotes point in ∂M indicated by the green dot ($\in \partial Q$) and the direction denoted by the green arrow on Left.

The invariant curve going through x in Fig. 17.11

17.21 How T transforms curves in ∂Q

Consider a curve $\varphi = \psi(r)$ in ∂M to understand how T maps this. After T let us write this curve becomes $\varphi_1 = \psi_1(r_1)$. We can write

$$\varphi_1(r, \varphi) = \psi_1(r_1(r, \varphi)), \tag{17.21}$$

Its derivatives are obtained easily with the chain rule and the results summarized in **17.25** must lie in the strips. One in the pink strip must be the unstable manifold of T through x (i.e., $W^+(x)$) and that in the green strip the stable manifold of x.

17.22 Unstable manifold of T

In contrast to the smooth dynamical systems, billiards are riddled with breaking due to collisions.[176] There is a transversal stable manifold that looks similar.

Figure 17.12: Unstable manifold of a Sinai billiard; the left figure explains why there are break points. [Fig. 7, 8 of DS II Bunimovich]

17.23 Change of the next collision by position change

Let us calculate one step $x \to x_1$ in detail.

First, let us study the changes in r_1 and φ_1 when r is changed by dr (Fig. 17.13).

If we keep φ and change the first collision position slightly by dr, due to the change of the normal directions of the reflecting surface, the direction of the reflected trajectory changes its angle by kdr (the purple angle). It takes τ fo the particle to reach the next collision point from the last collision, so

$$kdr\tau, \tag{17.22}$$

[176] Actually, it is usually made of many continuous components. Here, only one such component is illustrated.

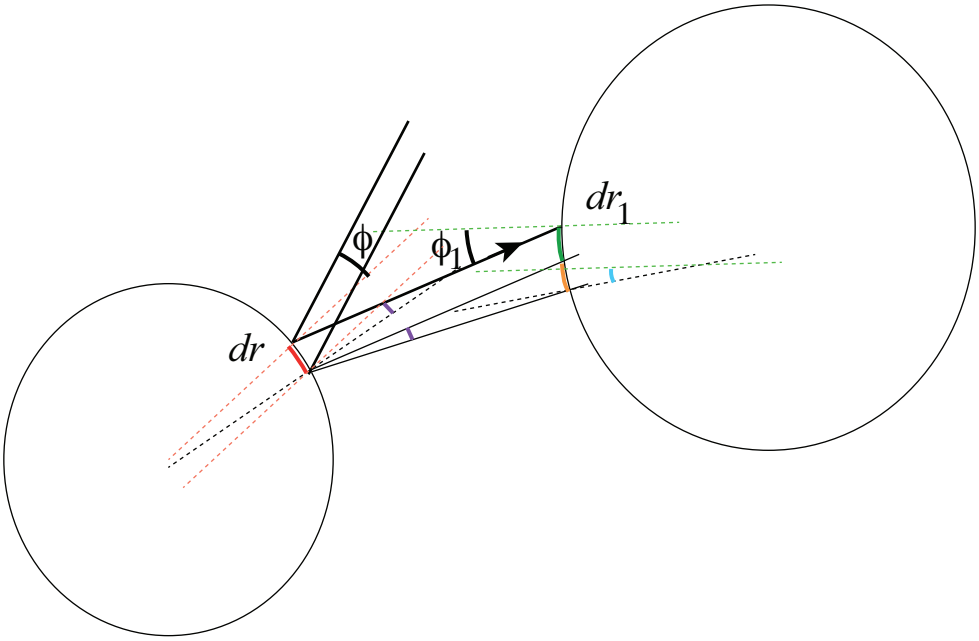

Figure 17.13: A propagation front and the velocities: change due to r

where k is the curvature of the boundary at the first collision point, is the displacement of the collision point perpendicular to the incidence direction. However, this direction makes angle φ_1 with the tangent direction of the new colliding surface. Thus, we need the length of te orange segment, which is

$$k dr \tau / \cos\varphi_1. \tag{17.23}$$

dr_1 has the green portion due to ther simple parallel displacement of the trajectory due to dr. The displacement distance is $dr\cos\varphi$. Thus, when this is projected on the second surface the displacement must be

$$dr\frac{\cos\varphi}{\cos\varphi_1}. \tag{17.24}$$

Thus the answer for dr_1 is the green and orange segments added, but we must worry about the sign. If dr is in the counterclockwise direction, dr_1 must be clockwise, so they should have opposite signs:

$$dr_1 = -dr\left(\frac{\cos\varphi}{\cos\varphi_1} + \frac{\tau k}{\cos\varphi_1}\right). \tag{17.25}$$

The change of the incidence angle to the second body consists of two parts: the blue angle due to the change of the normal direction due to displacement dr_1 and

the purple angle due to the change of the direction of the incidence ray (due to dr on the first body). The former is $k_1 dr_1$, where k_1 is the curvature at the new collision point. The purple portion is obviously kdr, which reduces φ_1. Therefore,

$$d\varphi_1 = -k_1 dr \left(\frac{\cos\varphi}{\cos\varphi_1} + \frac{\tau k}{\cos\varphi_1} \right) - kdr. \tag{17.26}$$

We also should consider the change in τ. This is clearly

$$d\tau = dr_1 \sin\varphi_1 - dr \sin\varphi. \tag{17.27}$$

17.24 Change of the next collision by angle change

Next, let us study the changes in r_1 and φ_1 when φ is changed by $d\varphi$ (Fig. 17.14).

If we keep r and change the first collision incidence angle slightly by $d\varphi$, the direction of the reflected trajectory changes with the same amount but in the opposite direction. It takes τ fo the particle to reach the next collision point from the last collision, so the particle to reach the next collision point from the last collision, so $d\varphi\tau$ is the displacement of the collision point perpendicular to the incidence direction. However, this direction makes angle φ_1 with the tangent direction of the new colliding surface. Thus, the green length $= dr_1$ is

$$dr_1 = -\tau d\varphi / \cos\varphi_1. \tag{17.28}$$

The incidence angle to the new boundary changes by the red angle due to the change of the direction of the trajectory, but the collision point is displaced by dr_1, so the normal direction changes by the orange angle: $k_1 dr_1$. Both contribute in the same direction, so

$$d\varphi_1 = \frac{k_1\tau}{\cos\varphi_1} d\varphi - d\varphi = -d\varphi \left(1 + \frac{k_1\tau}{\cos\varphi_1} \right). \tag{17.29}$$

We also have

$$d\tau = \tan\varphi_1 d\varphi. \tag{17.30}$$

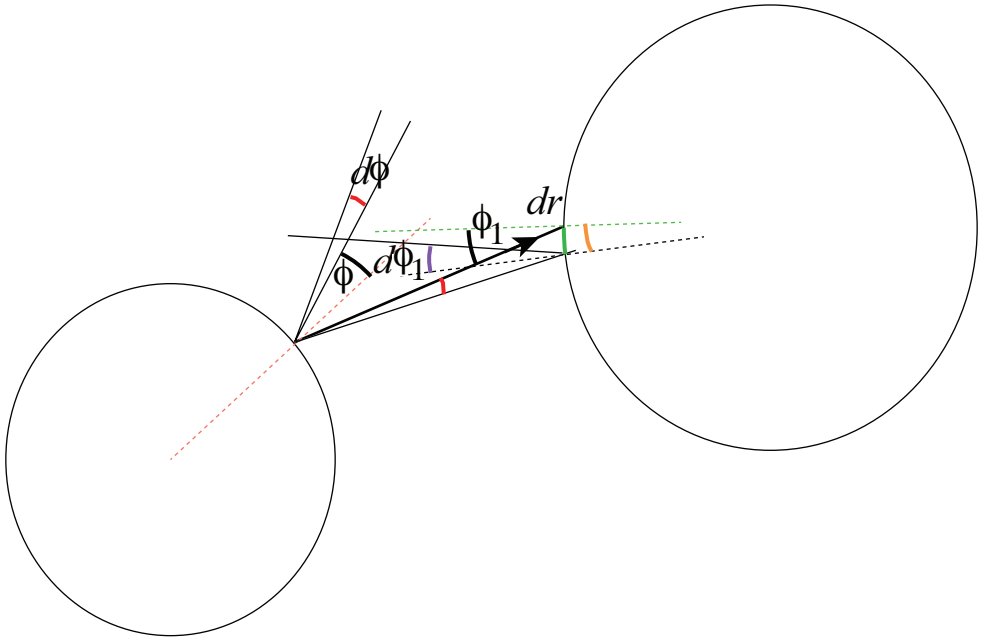

Figure 17.14: A propagation front and the velocities: change due to r

17.25 Summary of derivatives

We may summarize the results of **17.23** and **17.24** as follows:

$$\begin{pmatrix} \frac{\partial r_1}{\partial r} & \frac{\partial r_1}{\partial \varphi} \\ \frac{\partial \varphi_1}{\partial r} & \frac{\partial \varphi_1}{\partial \varphi} \end{pmatrix} = \begin{pmatrix} -\left[1+\frac{\tau k}{\cos\varphi}\right]\frac{\cos\varphi}{\cos\varphi_1} & -\frac{\tau}{\cos\varphi_1} \\ -k_1\left[1+\frac{\tau k}{\cos\varphi}\right]\frac{\cos\varphi}{\cos\varphi_1}+k & -\left[1+\frac{\tau k_1}{\cos\varphi_1}\right] \end{pmatrix}. \tag{17.31}$$

17.26 Kolmogorov-Sinai entropy of Sinai billiard: calculation

To compute h_T we need $\partial r_1/\partial r$. We differentiate $r_1 = r_1(r, \psi(r))$ (recall the remark at the end of **17.26**. Since $r_1 = r_1(r, \psi(r))$:

$$\frac{dr_1}{dr} = \frac{\partial r_1}{\partial r} + \frac{\partial r_1}{\partial \varphi}\frac{d\psi}{dr}. \tag{17.32}$$

Also, since

$$\varphi_1(r, \psi(r)) = \psi_1(r_1(r, \psi(r))), \tag{17.33}$$

$$\frac{\partial \varphi_1}{\partial r} + \frac{\partial \varphi_1}{\partial \psi}\frac{d\psi}{dr} = \frac{d\psi_1}{dr_1}\left(\frac{\partial r_1}{\partial r} + \frac{\partial r_1}{\partial \psi}\frac{d\psi}{dr}\right). \tag{17.34}$$

Therefore, we can solve

$$\frac{d\psi_1}{dr_1} = \frac{\frac{\partial\varphi_1}{\partial r} + \frac{\partial\varphi_1}{\partial\varphi}\frac{d\psi}{dr}}{\frac{\partial r_1}{\partial r} + \frac{\partial r_1}{\partial\varphi}\frac{d\psi}{dr}}. \tag{17.35}$$

(17.32) reads with (17.25) and (17.28)

$$\frac{dr_1}{dr} = -\left(\frac{\cos\varphi}{\cos\varphi_1} + \frac{\tau k}{\cos\varphi_1}\right) + \frac{\tau}{\cos\varphi_1}\frac{d\psi}{dr} \tag{17.36}$$

$$= -\frac{\cos\varphi}{\cos\varphi_1}\left(1 + \frac{\tau}{\cos\varphi}\left(k + \frac{d\psi}{dr}\right)\right). \tag{17.37}$$

We must compute $d\psi/dr$.

$$\frac{d\psi_1}{dr_1} = \frac{-k_1\left(\frac{\cos\varphi}{\cos\varphi_1} + \frac{\tau k}{\cos\varphi_1}\right) - k - \left(1 + \frac{k_1\tau}{\cos\varphi_1}\right)\frac{d\psi}{dr}}{-\left(\frac{\cos\varphi}{\cos\varphi_1} + \frac{\tau k}{\cos\varphi_1}\right) - \frac{\tau}{\cos\varphi_1}\frac{d\psi}{dr}} \tag{17.38}$$

$$= k_1 + \frac{k + \frac{d\psi}{dr}}{\left(\frac{\cos\varphi}{\cos\varphi_1} + \frac{\tau k}{\cos\varphi_1}\right) + \frac{\tau}{\cos\varphi_1}\frac{d\psi}{dr}} \tag{17.39}$$

$$= k_1 + \frac{k + \frac{d\psi}{dr}}{\frac{\cos\varphi}{\cos\varphi_1} + \frac{\tau}{\cos\varphi_1}\left(k + \frac{d\psi}{dr}\right)} \tag{17.40}$$

$$= k_1 + \frac{\cos\varphi_1}{\cos\varphi}\frac{k + \frac{d\psi}{dr}}{1 + \frac{\tau}{\cos\varphi}\left(k + \frac{d\psi}{dr}\right)} \tag{17.41}$$

$$= k_1 + \frac{\cos\varphi_1}{\cos\varphi}\frac{1}{\frac{\tau}{\cos\varphi} + \frac{1}{k + \frac{d\psi}{dr}}}. \tag{17.42}$$

Notice that this is a recurrence relation:

$$\frac{d\psi_n}{dr_n} = k_n + \frac{\cos\psi_n}{\cos\psi_{n-1}}\frac{1}{\frac{\tau_{n-1}}{\cos\psi_{n-1}} + \frac{1}{k_{n-1} + \frac{d\psi_{n-1}}{dr_{n-1}}}}. \tag{17.43}$$

The result of this recursion gives a continued fraction expression of $d\psi/dr$ required in (17.32). We can fairly accurately evaluate this numerically.

17.27 H in the small R limit

Friedman et al.[177] actually evaluated and conjectured $-H/\log R \to 2$ in the small R limit. Actually, they proved this value to be in $(1.5, 2]$ and numerically obtained the upper limit value 2.[178]

17.28 Billiards with scatters with finite potentials or soft billiards

Baldwin[179] considered an 'optical' system or the muffin-tin potential system with potential U (measured in kinetic energy):

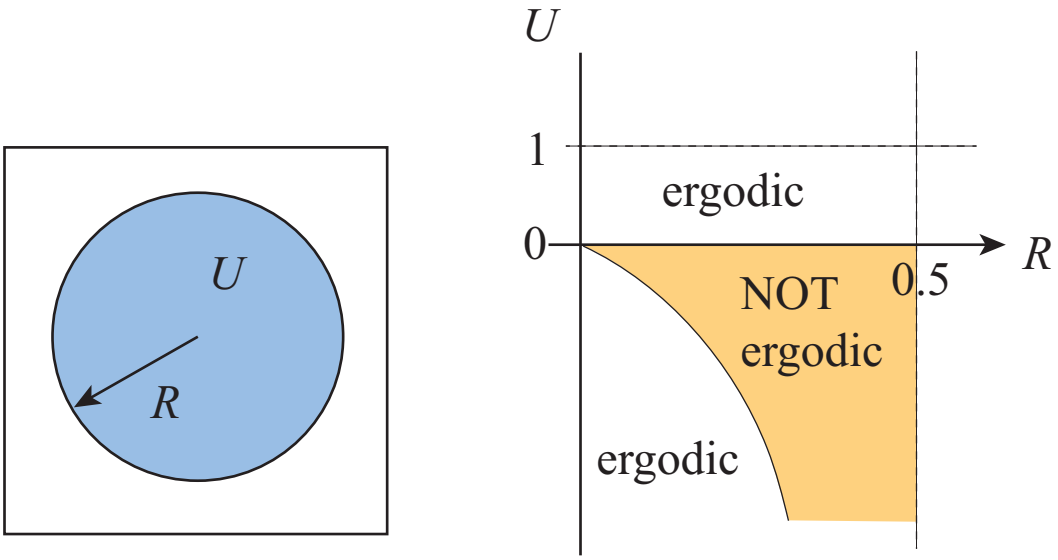

Figure 17.15: The table with U and the phase diagram; the non-ergodicity of the colored region is proved, but ergodicity of the remaining regions is a conjecture based on simulations. The lower bondary curve of the colored region is $U = 1 - 1/(1-2R)^2$.

In the nonergodic region we see elliptic fixed points.

[177] B. A. Friedman, Y. Oono and I. Kubo, PRL 52 709 (1984). See B. A. Friedman, UIUC Physics thesis 1985.

[178] $d(d-1)$ is the general formula: N Chernov, Entropy Values and Entropy Bounds (2006) is a good review): people.cas.uab.edu/~mosya/papers/hb.pdf.

[179] P. R. Baldwin, Soft billiard system, Physica D 29, 321 (1988). See P. R. Baldwin, UIUC Physics thesis 1987.